*Journal of Applied Electrochemistry* **34**: 849–856, 2004.



# Electrochemical aspects of pyrrhotite and pentlandite in relation to their flotation with xanthate. Part-I: Cyclic voltammetry and rest potential measurements

A. KHAN and S. KELEBEK*
*Department of Mining Engineering, Goodwin Hall, Queen's University, Kingston, Ont., Canada K7L 2N6*
*(*author for correspondence, e-mail: kelebek-s@mine.queensu.ca)*

Received 20 September 2003; accepted in revised form 17 March 2004

*Key words:* flotation selectivity, oxidation, pentlandite, pyrrhotite, rest potentials, xanthate

**Abstract**

Separation of pyrrhotite from pentlandite is highly important in flotation practice of massive nickel sulphide ores. Flotation reactivity of these minerals was studied using cyclic voltammetry and rest potential measurements, which included dissolved oxygen concentration and butyl xanthate addition as the main parameters at a solution pH of 9.2.

Under the experimental conditions used, the voltammograms, obtained in the absence and presence of xanthate (at 0.1 mol $m^{-3}$) and dissolved oxygen, provided no direct evidence for any anodic peaks that can be associated with xanthate electroadsorption or its possible transformation to dixanthogen, as an agent of superior hydrophobicity. However, the current densities corresponding to the most prominent anodic potential for pyrrhotite were noticeably lower in the presence of xanthate, suggesting its involvement in the formation of a partially passivating film.

According to results of rest potential measurements, formation of dixanthogen will be common to both of these minerals in oxygen-saturated solutions to promote their bulk flotation. However, under oxygen-deficient conditions in the presence of xanthate, pyrrhotite develops rest potentials that are much lower than the equilibrium potential for dixanthogen formation. Since dixanthogen formation is essential for pyrrhotite floatability, controlling the dissolved oxygen level and potential in the pentlandite–pyrrhotite flotation environment at low levels is expected to promote selective flotation of pentlandite, which has been demonstrated independently.

## 1. Introduction

Massive nickel sulphide ores have a generically complex mineralogy containing pentlandite (Pn, $(Ni_{4.5}Fe_{4.5})S_8$) that is in major association with pyrrhotite (Po, $Fe_7S_8$) and chalcopyrite (Cp, $CuFeS_2$). A pentlandite concentrate is the primary source of desirable nickel, cobalt and precious metals, while pyrrhotite itself is the primary source of undesirable sulphur although it also contains some nickel (e.g., 0.70–1.0%). There are continuous efforts to minimize the amount of sulphur input to smelters as part of overall sulphur dioxide abatement programs. This requires efficient separation of pyrrhotite from the nickel and copper concentrates. Flotation is the main separation method used in processing of such ores.

Oxidation constitutes a central part of the electrochemical reactivity of sulphide minerals in flotation systems. Alekseeva [1] reported that pyrrhotite oxidation is related to its sulphur-iron ratio. She observed an increase in the surface oxidation with increasing sulphur to iron ratio although depression of pyrrhotite was apparently unaffected. In the presence of xanthate, using higher levels of aeration, flotation recoveries were improved as compared to low levels of aeration. In contrast, it was also reported that, under certain conditions, selective flotation of pentlandite and chalcopyrite can be achieved as a result of selective oxidation of pyrrhotite through pre-aeration of slurries [2]. These observations suggest that behaviour of pyrrhotite is highly sensitive to small changes in flotation conditions (e.g., amount of xanthate and aeration).

Electrochemical methods provide useful information on oxidizing/reducing characteristics of sulphide minerals. Cheng et al. [3], using electrochemical techniques, reported that, under an atmosphere of oxygen, pyrrhotite showed a strong anodic response while chalcopyrite remained virtually unaffected when these minerals are brought into contact with mild steel, the material typically used as grinding media in processing. They further indicated that the conditions favourable for xanthate oxidation promoted chalcopyrite flotation. Oxidation products on sulphide minerals include hydroxides, oxides and oxy-sulphides [4]. When effectively formed, these surface species induce hydrophilicity and are responsible for depression of sulphide minerals in flotation [5]. Miller et al. [6] used cyclic voltammetry and contact angle measurements under potential control to study the low potential hydrophobic state of pyrite in amyl xanthate flotation using nitrogen in place of air.

In an adsorption study, Fornasiero et al. [7] reported formation of dixanthogen as the only surface species ultimately responsible for flotation of pyrrhotite, an observation that has been frequently noted by others. Bozkurt et al. [8], using the rest potential technique suggested the formation of dixanthogen on pentlandite and retardation of its formation on pyrrhotite in a mixed mineral system. More recently, Buswell and Nicol [9] investigated the electrochemical behaviour of pyrrhotite and conditions of its improved flotation and copper activation as a case that is relevant for the South African low-grade nickel sulphide ores, where flotation of all sulphides for an efficient bulk flotation is the main issue.

An equally important aspect of nickel sulphide ore processing in North America relates to problems of flotation selectivity. In this study, electrochemical characteristics of pyrrhotite and pentlandite were investigated and their interactions with the xanthate examined in the presence and absence of dissolved oxygen. Results obtained are discussed for their implication in the flotation separation behaviour of pentlandite and pyrrhotite.

## 2. Experimental details

### 2.1. *Methods and procedures*

The electrochemical setup involved a standard 3-electrode cell using a selected sulphide mineral electrode as the working electrode, saturated calomel electrode as the reference electrode and a bright platinum plate (0.01 m × 0.01 m) as the counter electrode. In all experiments, the working electrode was kept stationary while the electrolyte solution was stirred continuously. A schematic diagram of the experimental setup used for both cyclic voltammetry and rest potential studies is given in Figure 1. For the electrochemical measurements, a PC3 potentiostat card with CMS 105 interface from Gamry Instrument Inc. was used. Potentials are reported against the standard hydrogen electrode.

Cyclic voltammetry experiments were conducted on pyrrhotite and pentlandite in sodium borate solutions of 50 mol $m^{-3}$ (0.05 M) between potentials of −0.56–1.040 V and at a scan rate of 0.01 V $s^{-1}$. The polarization of the electrode was started from its rest potential and continued in the cathodic direction up to the negative vertex potential and the potential scan was then reversed in the anodic direction and continued until it reached the positive vertex potential. This was followed by a reversed potential scan to get a complete cycle. For analytical purposes, the initial scan between the rest potential and negative vertex potential were discarded because the current response in this region could be dominated by the reduction of the species produced during the polishing of the electrode.

For rest potential measurements, the solutions were oxygenated or deoxygenated before xanthate addition at

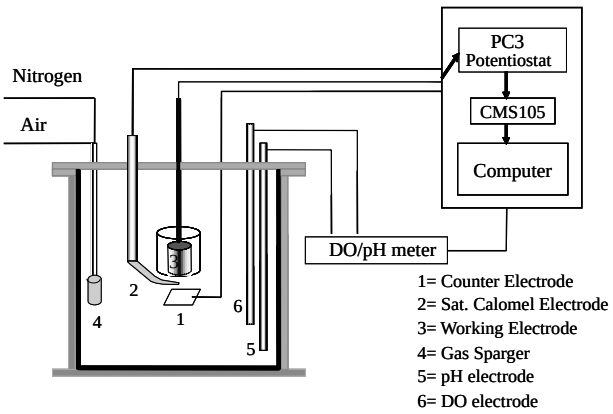


*Fig. 1.* A schematic diagram of the experimental setup for cyclic voltammetry and rest potential experiments.

0.1 mol $m^{-3}$ ($10^{-4}$ M). Following addition of the xanthate, the working electrode was freshly polished, rinsed and immediately dipped into the solution and the measurements were taken. Electrode potential was monitored as a function of time.

### 2.2. *Materials and electrode preparation*

The working electrodes were prepared from mineral samples of high purity which were cut into easily measurable geometric shapes. The samples of pyrrhotite and pentlandite came from the Sudbury and Manitoba mining regions of Canada, respectively. Analytical work on the samples showed no significant impurity in the pyrrhotite (0.17% Cu and 0.02% Ni). However, X-ray diffraction analysis of pentlandite samples indicated the presence of some pyrrhotite, pyrite and low nickel levels (0.29% Cu and 14.6–34.1% Ni). The specimen that appeared to have no visible inclusions at its surface was selected as the electrode material for this sample. In addition, a synthetic pentlandite was prepared using the appropriate methods [10–12]. This sample was needed to compare its voltammetric behaviour with that of the natural pentlandite sample. However, due to the porous nature of the synthetic sample obtained and its potential risk of contamination during the polishing stage, the majority of experiments were carried out using the natural pentlandite specimen only.

Pre-cut mineral specimens of electrodes were moulded in resin (105 Epoxy with 205 Hardener, Gougcon West System) carrying a conductive electric wire at the top via silver epoxy to reduce the contact resistance. The electrode was thoroughly rinsed with a strong jet of double distilled water during and after the polishing stage (using a 400-grit and 800-grit silicon carbide paper). A final rinsing was carried out just before its transfer to the electrochemical cell. Plastic surgical gloves were used during all experiments.

Compressed air and ultra pure compressed nitrogen were used to control the dissolved oxygen concentration in the cell. Sodium *n*-butyl xanthate was used as a collector, which was synthesized according to suggested

procedures [13]. The xanthate crystals were stored in a fridge and under petroleum ether to avoid contact with atmospheric oxygen.

## 3. Results and discussion

### 3.1. *Cyclic voltammetry*

#### 3.1.1. *Pyrrhotite system*

Figure 2 shows the cyclic voltammetry results of pyrrhotite. Each working electrode was tested under four different electrolyte conditions, namely the presence and absence of dissolved oxygen and xanthate, respectively, as indicated in the figure legend. On the anodic scan, two oxidation current peaks (Po-1 and Po-2) can be noted, whereas, on the cathodic scan, one prominent reduction current peak (Po-3) is present. The peak Po-1 started at about −0.05 V and continued in a wide potential range up to 0.11 V. No significant difference in the current density was observed with regard to the electrolyte composition. The presence or absence of dissolved oxygen or xanthate appears to have no effect on the electrochemical reactivity of the surface species produced in this potential region. The current peak starting at about −0.05 V (Po-1) is attributable to the following electrochemical reaction;

$$\mathrm{Po[Fe_{1-x}S] + 3yOH^- = Po[Fe_{1-(x+y)}S + (y-z)Fe(OH)_3] + zFe(OH)_3 + 3ye^-} \quad (1)$$

where $(Fe_{1-x})S$ is shown as an iron deficient surface of pyrrhotite with $x$ typically increasing up to 0.2. It reacts in the alkaline solution and forms a surface product with even greater iron-deficiency, which is accompanied by formation of ferric hydroxide. For this oxidation stage, excess sulphur has been considered to be in the form of elemental sulphur [14] and polysulphide [15]. Ferric hydroxide as an oxidation product is known to largely precipitate on the pyrrhotite surface. The resulting surface of pyrrhotite is considered to have a heterogeneous character, showing a patch-wise surface structure [16]. The pyrrhotite voltammogram recently reported by Buswell and Nicol [9] did not indicate a peak in this region in their first scan in the anodic direction. There was only a relatively small anodic current plateau from 0.20 to 0.50 V although subsequent anodic scans produced two peaks in the same potential range. In the present work, further increase in scanning potential in the intermediate range did not result in an additional distinct current peak, until the potential scan has reached about 0.50 V, where a new anodic current peak appeared (Po-2) and reached its maximum current density at 0.75 V. This anodic process is considered to involve oxidation of the sulphide part of pyrrhotite in addition to formation of ferric hydroxide [9, 14]. The overall oxidation reaction leading to sulphate formation is shown below:

$$\mathrm{Po[FeS_{1.13}] + 4.52H_2O = Po[Fe(OH)_3] + 1.13SO_4^{2-} + 9.04H^+ + 9.78e^-} \quad (2)$$

As noted above, the presence of xanthate had no apparent effect on the starting potential of the peak. However, the maximum peak potential shifted to 0.80 V and reduction in the maximum current density was observed. At the higher dissolved oxygen level, in the presence of xanthate, the current density is consistently higher indicating that the extent of the surface oxidation reaction is correspondingly greater. On the other hand, the current density is lower in the presence of xanthate regardless of the concentration level of dissolved oxygen. Higher oxygen concentration facilitates oxidation in both cases. The present study indicates that, in the presence of xanthate, the current flow corresponding to the oxidation of pyrrhotite surface is somewhat inhibited for both levels of oxygen in the electrolyte.

These effects that are evidently caused by the presence of xanthate should have their voltammetric origin in lower potential regions as well but they are, in a way, masked in view of the dominant electrochemical reactivity of pyrrhotite and relatively weak interaction of iron species with xanthate. That an anodic peak for xanthate adsorption has not been observed for pyrrhotite agrees with the recent observations by Buswell and Nicol [9]. However, they demonstrated enhanced anodic currents at lower potentials in the presence of xanthate only when its concentration was increased 100 times.

On the other hand, xanthate is considered to form iron hydroxy xanthates [17]. This is an area investigated in detail by Wang et al. [18], who using thermodynamic stability diagrams, demonstrated that ferric dihydroxy xanthate is a highly stable species under alkaline conditions at potentials lower than the stability domain of dixanthogen. Although such a surface species will

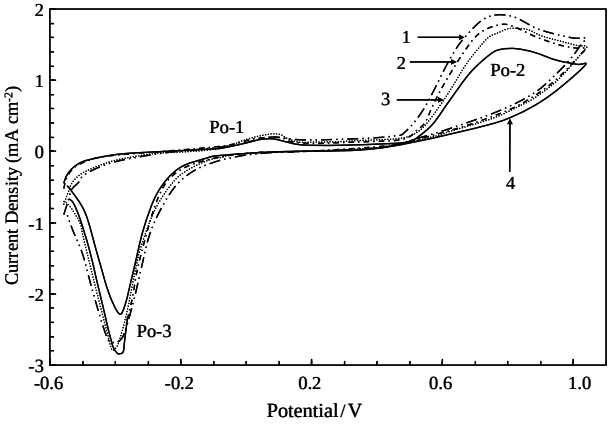


*Fig. 2.* Cyclic voltammograms of pyrrhotite electrode under various conditions (pH 9.2) with a scan rate of 10 mV $s^{-1}$ (numbers indicate concentrations of dissolved oxygen (DO) and sodium *n*-butyl xanthate (X), (1) DO = 8.15 $mgl^{-1}$, X = 0 mol $m^{-3}$, (2) DO = 0.1 $mgl^{-1}$, X = 0 mol $m^{-3}$, (3) DO = 8.15 $mgl^{-1}$, X = 0.1 mol $m^{-3}$, (4) DO = 0.1 $mgL^{-1}$, X = 0.1 mol $m^{-3}$).

have a small hydrophobicity level it is considered to be a favourable site to accommodate dixanthogen. It can form during the very initial phase of pyrrhotite reaction through the adsorption of xanthate ions even without charge transfer. Ferrous species are much more soluble than ferric species. An appreciable amount of soluble species can be released into solution even at a pH of 9 at moderate redox levels [7]. As a result of oxidation, some ferrous species may be released from pyrrhotite interact in solution and are transformed into other species depending on the solution chemistry to eventually form positive surface sites in favourable areas of pyrrhotite by readsorption. Initial adsorption of xanthate then proceeds at these specific sites as a result of electrostatic interaction:

$$\mathrm{Po[Fe(OH)]^{+} + X^{-} \rightarrow Po[Fe(OH)]^{+} \cdot X^{-} \rightarrow Po[Fe(OH)X]} \quad (3)$$

Once xanthate species are physically on pyrrhotite, which is considered to have a heterogeneous and reactive surface, chemisorption forces are likely to come into action as well. These ferrous based species are considered to be metastable. More stable forms of ferric counterparts can follow through transformation steps, for example:

$$\mathrm{Po[Fe(OH)X] + OH^{-} \rightarrow Po[Fe(OH)_2X] + e^{-}} \quad (4)$$

Further adsorption of xanthate can lead to dixanthogen formation:

$$\mathrm{Po[Fe(OH)_2X] + X^{-} \rightarrow Po[Fe(OH)_2X - X] + e^{-}} \quad (5)$$

$$\mathrm{Po[Fe(OH)_2X - X] + X^{-} \rightarrow Po[Fe(OH)_2X - X_2] + e^{-}} \quad (6)$$

Development of appreciable hydrophobicity on pyrrhotite surfaces is observed in the potential range of 0.10–0.125 V [19]. This is broadly in agreement with the current peak position recently reported [9].

According to thermodynamic calculations ferric hydroxide and dixanthogen can co-exist as stable phases. However, surface structural details are not well understood. It is reasonable to visualize dixanthogen as being fixed at the ferric dihydroxy xanthate sites of the surface, as depicted in reaction (6). It is also proposed that the dixanthogen acquires its enhanced stability by migrating onto sulphur-rich sites of pyrrhotite surface. As noted earlier, pyrrhotite is an iron-deficient (relatively sulphur-rich) sulphide by its nature, and this iron-deficiency increases as a result of its oxidation. This phenomenon that is considered to precede possible formation of elemental sulphur has been linked with self-induced hydrophobicity and collectorless flotation behaviour of sulphide minerals [20], especially when the elemental sulphur liberation does occur. Many sulphide minerals are known to exhibit this property including pyrrhotite and pentlandite [21–22].

The cathodic current peak designated as Po-3 in Figure 2 is relatively broad, starting between 0.20 and 0 V and then reaching a maximum current density around −0.40 V. As noted above, xanthate is known to adsorb on pyrrhotite in this initial potential range (in anodic direction), which then acquires a hydrophobic character [19]. However, there is no evidence of xanthate desorption under reducing conditions since the cathodic sweeps obtained in the presence and absence of xanthate are practically the same. Overall, this potential range is attributable to reduction of the ferric species that had formed during anodic scans. The ferric species reduced predominantly involves ferric hydroxide in addition to some residual xanthate derivatives of ferric hydroxide discussed earlier. The reversal of another surface reaction involving oxidation of sulphur is also relevant to note here. Some details on reduction of sulphur species to sulphide have been reported in recent work [8]. There appears to be no cathodic peak that could be specifically attributable to the reduction of dixanthogen. This is consistent with the view that its formation does not involve a dominant electrode reaction. Dixanthogen that may have formed by another mechanism is believed to be relatively low and is likely to have been lost to the solution following destabilization of an underlying site such as for the metastable sulphur noted above. The loss of stability does not need to be taking place during the cathodic scan. It can take place earlier during the anodic scan at high potentials.

Figure 2, also shows that the reduction current density is relatively higher than the anodic current densities. This suggests that the electrode surface has been altered by oxidation to a greater degree than indicated by the summation of anodic current densities. In view of the reactivity of pyrrhotite and the complexity of its oxidation reactions this is not surprising. For example, oxidation of the sulphide part of pyrrhotite at and beyond 0.75 V to soluble species such as sulphate is likely to expose more iron in the surface, which can then be oxidized to ferric hydroxide, thereby contributing to the total amount of ferric species at the electrode surface and subsequently to their reduction current density.

### 3.1.2. *Pentlandite system*

Figure 3 shows a comparison of cyclic voltammograms of the natural and synthetic samples of pentlandite in air saturated and buffered electrolyte solutions containing no xanthate. The voltammograms from both electrodes are almost identical in the potential range relevant to flotation practice. In contrast to the case with the pyrrhotite electrode tested, under the same experimental conditions, there is only one anodic current peak and one cathodic current peak in both cases. However, the oxidation potential for the synthetic pentlandite is higher by about 0.20 V. This suggests that synthetic pentlandite is somewhat passivated and more resistant to oxidation. Apparent dissimilarity may be a reflection

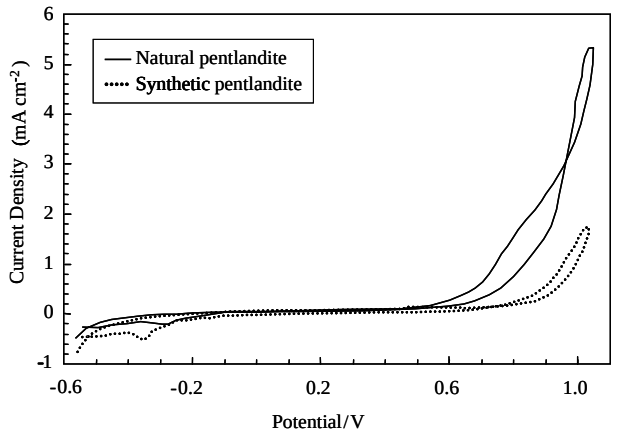


*Fig. 3.* Cyclic voltammograms of natural and synthetic pentlandite in oxygen saturated and buffered electrolyte solutions (pH 9.2) scanned at 10 m V $s^{-1}$.

of different stoichiometries involved in each case as well as the impurities associated with the natural pentlandite. Natural pentlandites usually show a variety of stoichiometries [23].

Figure 4 shows the cyclic voltammograms for pentlandite under conditions similar to those applied for pyrrhotite. Neither the change in the current densities, nor the starting peak potentials seems to be dependent on the dissolved oxygen concentration, and on the presence or absence of xanthate. As in the case of the second anodic current peak of pyrrhotite, the most prominent anodic current peak of pentlandite starts at about 0.50 V and continues with a gradual increase in the current merging into another current peak before the scan is reversed. In this region, the extent of overall increase in the current density is much greater than the case observed for pyrrhotite. In view of the ferrous nature of pentlandite ($Ni_{4.5}Fe_{4.5})S_8$, the anodic peak in this region can be associated with formation of ferric

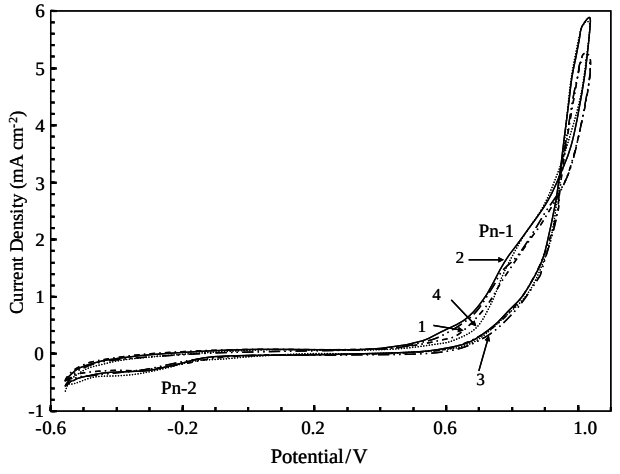


*Fig. 4.* Cyclic voltammograms of pentlandite electrode under various conditions (pH 9.2) with a scan rate of 10 m V $s^{-1}$ (see Figure 2 caption for meaning of numbers).

and nickel hydroxide and the oxidation of sulphide species as given below;

$$Pn[(Fe_{4.5}Ni_{4.5})S_8] + 22.5OH^- \rightarrow Pn[(4.5Fe(OH)_3 + (4.5 - x)Ni(OH)_2 + 8S] + xNi(OH)_2 + 22.5e^- \quad (7)$$

$$Pn[(Fe_{4.5}Ni_{4.5})S_8] + 54.5OH^- \rightarrow Pn[(4.5Fe(OH)_3 + (4.5 - x)Ni(OH)_2] + xNi(OH)_2 + 8SO_4^{2-} + 38.5e^- \quad (8)$$

In contrast to the prominent oxidation reactions evidently taking in this region, cathodic peaks are associated with much smaller currents. This is probably related to the soluble nature of some of the oxidation products formed (e.g., Equation 8).

In order to exhibit hydrophobicity, pentlandite must react with xanthate and assume its usual orientation. According to Senior and Trahar [5], this may occur in the range 0–0.05 V. The results in Figure 4 do not indicate an anodic peak associated either with the oxidation of this mineral or adsorption/oxidation of xanthate species. The initial adsorption step may not involve an electron transfer mechanism as discussed in the previous section for pyrrhotite. However, the apparent absence of an anodic current peak for oxidation of pentlandite within the moderate potential range of interest (e.g., −0.25 to +0.40 V) is surprising. Hodgson and Agar [21] reported anodic currents, one starting at a potential of −0.45 V SCE (about −0.205 V SHE) for the initial oxidation of their pentlandite electrode specimen. Such initial oxidation is considered to generate anodic sites on the mineral, most likely involving ($Ni^{2+}$), which are favourable for chemisorption of xanthate. This step is followed by dixanthogen formation at its favourable potential range. This is the view adopted here despite the absence of clear indications in the present work experimentally supporting it. Although further work is in progress in this area, the case for pentlandite is documented for a comparison with pyrrhotite under the same conditions.

### 3.2. *Rest potential measurements*

#### 3.2.1. *Pyrrhotite system*

Rest potential measurements were carried out with pyrrhotite electrodes under corresponding conditions of the voltammetric studies. Figure 5 shows the rest potential of pyrrhotite as a function of time up to 50 min. The rest potential profile of pyrrhotite is similar in the presence and absence of xanthate under oxygen-saturated conditions. The only notable difference is the magnitude of the potential change. The straight line represents the equilibrium potential for the transformation of xanthate to dixanthogen, which is around 0.125 V for *n*-butyl xanthate under the experimental conditions used. This value was calculated from the

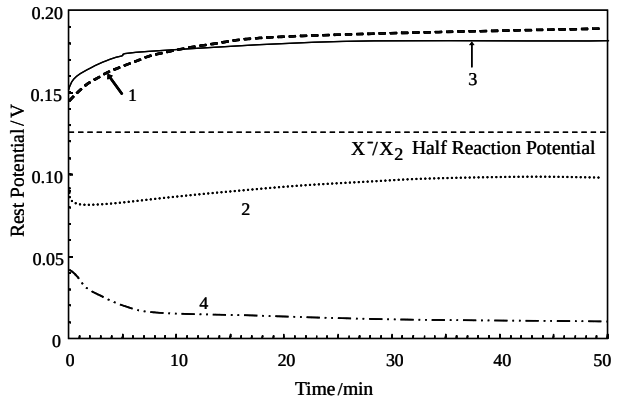


*Fig. 5.* Rest potential variation of pyrrhotite electrode under various conditions (pH 9.2) (see Figure 2 caption for meaning of numbers).

Nernst equation using an average standard half cell potential ($E^0$) value of −0.11 V for this reaction [24]. The rest potential is greater under these conditions at any particular time than the equilibrium potential for transformation of xanthate to dixanthogen. This suggests that the formation of dixanthogen on the pyrrhotite surface proceeds spontaneously.

When the dissolved oxygen concentration in the electrolyte is low, the rest potential of pyrrhotite in the presence of xanthate is significantly below the potential needed for $X^-/X_2$ transformation. This indicates that the formation of dixanthogen is not possible under oxygen-deficient conditions. When there is a negligible amount of oxygen in solution, the conversion xanthate-dixanthogen reaction is not supported since pyrrhotite is a poor catalyst for oxygen reduction.

### 3.2.2. *Pentlandite system*

Figure 6 shows the rest potential behaviour of pentlandite as a function of time. In the presence of oxygen, the rest potential of pentlandite is greater than the equilibrium potential for the xanthate/dixanthogen half reaction. This has also been observed for pyrrhotite. However, the initial rest potential for pentlandite is about 0.245 V compared to that of pyrrhotite at about 0.18 V. Therefore, in the presence of dissolved oxygen there is a greater driving force for the formation of dixanthogen on pentlandite than on pyrrhotite.

In the absence of dissolved oxygen and in the presence of xanthate, the rest potential of pentlandite decreased. However, during the initial period of the experiment, the rest potential, starting at 0.14 V, is still higher than the equilibrium potential for dixanthogen formation. This initial period is compatible with the time scale involved in reagent-mineral interaction in flotation practice. Thus, dixanthogen formation may still proceed on freshly generated pentlandite surfaces.

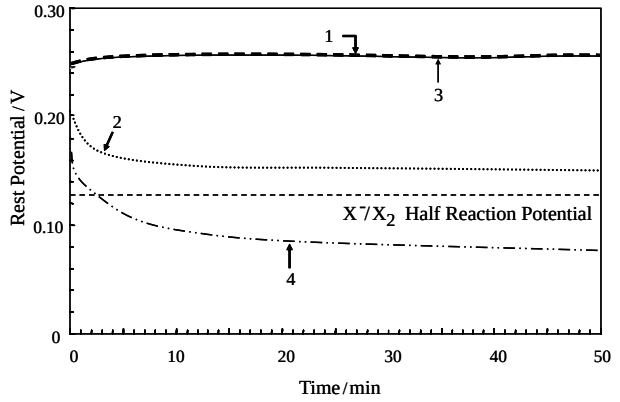


*Fig. 6.* Rest potential variation of pentlandite electrode under various conditions (pH 9.2) (see Figure 2 caption for meaning of numbers).

### 3.3. *Flotation selectivity under potential control*

Figure 7 shows the flotation selectivity between pentlandite and pyrrhotite. The case for potential control refers to a condition whereby the potential of the pulp was kept at relatively low levels, i.e., −0.095 to −0.055 V at initial stages and about −0.005 to 0 V at subsequent stages. This was achieved by using oxygen-deficient gas (maintained mostly using nitrogen) for flotation of a reground mixture of minerals. The samples employed in these tests originated from process streams consisting mainly of pyrrhotite-pentlandite middlings processed in a nickel–copper processing plant in the Sudbury region of Canada. The other case refers to a baseline condition whereby the potential continuously increases during flotation up to a level between 0.25 and 0.30 V due to the use of air as in usual practice. In both cases, the middlings were subjected to the same regrinding stage using mild steel grinding media in the pH range of 9–9.5 and were floated with isobutyl xanthate at about 0.1 mol $m^{-3}$. The regrinding step is essential for liberation of pentlandite from pyrrhotite since these two minerals are intimately associated with one another.

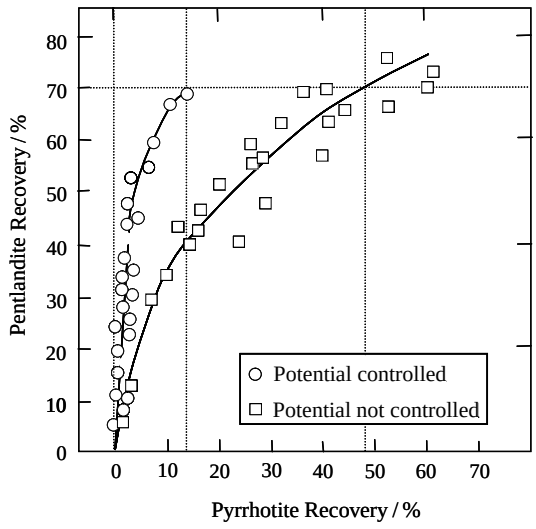


*Fig. 7.* Flotation selectivity between pentlandite and pyrrhotite following regrinding of their middlings in a steel mill at pH 9–9.5 (see text for details).

The case for potential control produces much better selectivity in favour of pentlandite recovery. This is a highly desirable outcome since the separation of a pentlandite-rich stream (i.e., concentrate) means much higher nickel grade in the concentrate. The first case achieves about 70% pentlandite recovery at only about 14% pyrrhotite recovery, compared to about 48% pyrrhotite recovery in the other case, thus eliminating about 34% pyrrhotite from the concentrate. This is highly significant as it represents about a 71% decrease in the recovery of pyrrhotite as the undesirable mineral component. Although flotation conditions in processing of related ores can be complex, involving many more variables than those in electrochemical studies, fundamental separation behaviour of these two minerals is in good agreement with the results obtained in this study, especially the results of the rest potential measurements. The discussion in the previous section was centred on conditions of dixanthogen formation. A difference in its kinetics of formation is possibly an important factor in the flotation results reported. On the other hand, while dixanthogen formation is highly important for pyrrhotite floatability it is believed to be not as important for pentlandite. Since the latter can develop anodic nickel sites which can support chemisorption of xanthate it may well be sufficient for its selective flotation. In either case, the occurrence of anodic half reactions is linked to their cathodic half reactions, which consist of dissolved oxygen reduction in both cases. Thus, the significant difference in oxygen reduction rate between pentlandite (faster) and pyrrhotite (slower) [25] is considered to have played an important role in flotation selectivity being in favour of pentlandite as demonstrated in Figure 7.

### 3.4. *Summary and conclusions*

Cyclic voltammetry and rest potential measurements were carried out with pentlandite and pyrrhotite electrodes in the presence and absence of dissolved oxygen and butyl xanthate. Under experimental conditions relevant to industrial operations (i.e., pH of 9.2 and collector dosage at 0.1 mol $m^{-3}$), cyclic voltammetry did not provide clear evidence for the formation of dixanthogen at the mineral surface. However, main electrochemical reactions involving formation of iron-deficient surface, ferric hydroxide/ferric dihydroxy xanthate, sulphur/sulphate were identifiable or reconcilable with the previous reported results. The current densities corresponding to the most prominent anodic potential for pyrrhotite were noticeably lower in the presence of xanthate regardless of dissolved oxygen concentration, suggesting its involvement in the formation of a partially passivating film. For pentlandite, there was practically no distinction in the voltammograms produced under the same conditions used for pyrrhotite. Rest potential measurements provided results that can be more directly related to the separation of these minerals. The formation of dixanthogen will be common to both minerals in oxygen-saturated solutions, promoting non-selective separation. However, under oxygen-deficient conditions in the presence of xanthate, pyrrhotite develops rest potentials that are much lower than the equilibrium potential for dixanthogen formation. Since dixanthogen formation is essential for pyrrhotite floatability, controlling the potential of the flotation environment below that level is expected to promote selective recovery of pentlandite. This has been demonstrated independently by results of batch flotation of pentlandite-pyrrhotite middlings.

## Acknowledgements

The authors wish to acknowledge the funding from Natural Sciences and Engineering Research Council of Canada (NSERC).

## References

1. R.K. Alekseeva, *Tsventy Metally* (*Non-Ferrous Metals*) **6**(3) (1965) 19.
2. S. Kelebek, The effect of oxidation on the flotation behaviour of nickel–copper ores, *in Proc. XVIII Int. Mineral Process. Congr.*, 1993, pp. 999–1005.
3. X. Cheng, I. Iwasaki and K.A. Smith, *Minerals Metall. Process* **16**(1), (1999) 69.
4. K.K. Das, A. Briceno and S. Chander, *Mineral Process. Extractive Metall. Rev.* **8** (1992) 229.
5. G.D. Senior and W.J. Trahar, *Int. J. Mineral Process.* **33** (1991) 321.
6. J.D. Miller, R. Plessis, D.G. Du Kotylar, X. Zhu and G.L. Simmons, The low potential hydrophobic state of pyrite in amyl xanthate flotation with nitrogen, *Preprint from SME Annual Meeting* (Feb. 28–Mar. 01, Salt Lake City, Utah, USA, 2000).
7. D. Fornasiero, M. Mentalti and J. Ralston, *J. Colloid Interface Sci.* **172** (1995) 467.
8. V. Bozkurt, Z. Xu and J.A. Finch, *Int. J. Mineral Process.* **52** (1998) 203.
9. A.M. Buswell and M.J. Nicol, *J. Applied Electrochem.* **32** (2002) 1321.
10. P.H. Ribbe, *Sulfide Mineralogy* (Min. Soc. America, Washington, 1974), 276 p.
11. O.P. Malik and R.A. Arnold, *Geol. Assoc. Can-Mineral Assoc. Can.*, Sudbury, (1971) 40.
12. K.C. Misra and M.E. Fleet, *Econ. Geol.* **68** (1973) 518.
13. S.R. Rao, *Xanthates and Related Compounds*, Marcel Dekker, 1972.
14. I.C. Hamilton and R. Woods, *J. Electroanal. Chem.* **118** (1981) 327.
15. M. Hodgson and G.E. Agar, *in* P.E. Richardson, S. Srinivasan and R. Woods (Eds.), *International Symposium on* '*Electrochemistry in Mineral and Metal Processing*' *Electrochemical Society*, 1984, pp. 185–201.
16. M. Hodgson and G.E. Agar, *Canadian Metall. Q.* **28**(3) (1989) 189.
17. P.J. Harris and N.P. Finkelstein, *Int. J. Mineral Process.* **2** (1975) 77.
18. X. Wang, K.S.E. Forssberg and N.J. Bolin, *Int. J. Miner. Process.* **27** (1989) 1.
19. R.H. Yoon, C.I. Basilio, M.A. Marticorena, A.N. Kerr and R. Stratton-Crawley, *Minerals Eng.* **8**(7) (1995) 807.

20. A.N. Buckley and R. Woods, *in* R. Woods, F.M. Doyle, P. Richardson (Eds.), *Electrochemistry in Mineral and Metal Processing IV* (The Electrochemical Soc., 1996) 96–6, pp. 1–12.
21. M. Hodgson and G.E. Agar, Electrochemical and flotation studies on pentlandite and pyrrhotite, *Preprint from SME-AIME Annual Meeting* (Feb. 24–28, New York, USA, 1985).
22. S. Kelebek, *Trans. Inst. Min. Metall.* **105** (1996) C75.
23. D.J. Vaughan and J.R. Craig, *Mineral Chemistry of Metal Sulfides* (Cambridge University Press, 1978), 493 p.
24. S. Chander, *Minerals and Metallurgical Processing* (August) (1988) 104.
25. D.A.J. Rand, *J. Electroanal. Chem.* **83** (1977) 19.